Biosensors and Bioelectronics 64 (2015) 664–670

Contents lists available at ScienceDirect

Biosensors and Bioelectronics

journal homepage: www.elsevier.com/locate/bios

Miniature multi-channel SPR instrument for methotrexate monitoring in clinical samples

Sandy Shuo Zhao [a], Natalia Bukar [a], Jacynthe L. Toulouse [a,c], Daniel Pelechacz [a], Robert Robitaille [b], Joelle N. Pelletier [a,c], Jean-François Masson [a,d,*]

[a] Département de Chimie, Université de Montréal, C.P. 6128 Succ. Centre-Ville, Montréal, QC, Canada H3C 3J7
[b] Département de Biochimie, Centre de Recherche, Hôpital Maisonneuve-Rosemont, 5415 Boulevard de l'Assomption, Montréal, QC, Canada H1T 2M4
[c] PROTEO, Canada
[d] Centre for Self Assembled Chemical Structures (CSACS), Canada

ARTICLE INFO

Article history:
Received 15 May 2014
Received in revised form
11 August 2014
Accepted 29 September 2014
Available online 2 October 2014

Keywords:
Biosensors
Surface plasmon resonance
Localized surface plasmon resonance
Gold nanoparticles
Therapeutic drug monitoring
Methotrexate

ABSTRACT

A multi-channel fully integrated SPR biosensor was applied for the analysis of an anti-cancer drug, methotrexate (MTX) as a potential analytical tool used in clinical chemistry laboratories for therapeutic drug monitoring (TDM). MTX concentrations in a patient's serum undergoing chemotherapy treatments can be determined by surface plasmon resonance (SPR) sensing using folic acid-functionalized gold nanoparticles (FA-AuNP) in competition with MTX for the bioreceptor, human dihydrofolate reductase (hDHFR) immobilized on the SPR sensor chip. To validate this biosensor, 13 nm FA-AuNP were shown to interact with immobilized hDHFR in the absence of MTX and this interaction was inhibited in the presence of MTX. The sensor was calibrated for MTX in phosphate buffer at different dynamic range by varying nanoparticle sizes (5, 13, 23 nm) and by modifying the K_d of the bioreceptor using wild-type and mutant hDHFR. Furthermore, initial binding rate data analyzes demonstrated quantitative and fast sensor response under 60 s. This MTX assay was subsequently adapted to a fully integrated multi-channel SPR system built in-house and calibrated in human serum with a dynamic range of 28–500 nM. The SPR system was applied to analyzes of actual clinical samples and the results are in good agreement with fluorescence polarization immunoassay (FPIA) and LC–MS/MS. Finally, the prototype system was tested by potential clinical users in a hospital setting at the biochemistry laboratory of a Montreal hospital (*Hôpital Maisonneuve-Rosemont*).

1. Introduction

Methotrexate (4-amino-10-methylpteroylglutamic acid) is an antifolate used for treating different types of cancer (Walling, 2006). MTX is a chemical analog of folic acid that tightly inhibits hDHFR (EC 1.5.1.3), a ubiquitous cytosolic enzyme. hDHFR reduces its substrate, 5,6-dihydrofolate, to 5,6,7,8-tetrahydrofolate which constitutes a major cofactor for the biosynthesis of purines and thymidine which are essential for the replication of DNA in cell division. Thus, MTX treatment abrogates rapidly dividing cancerous cells (Ackland and Schilsky, 1987).

High-dose MTX infusions are susceptible to result in symptoms of toxicity such as myelosuppression and gastrointestinal mucositis. MTX clearance depends greatly on the proper renal function of the patient. The risk of a potentially fatal toxicity associated with high-dose MTX increases with renal impairment because slower clearance of MTX prolongs duration of exposure in the patient (Blum et al., 2002). Dose adjustment in MTX chemotherapy is routinely undertaken to address the large variability in inter-individual pharmacokinetics where concentrations can vary over a 5-fold range from one patient to another using a single fixed dose (Graf et al., 1994; Pignon et al., 1994). It is important to highlight that during treatment, circulating MTX concentration can fluctuate over 5 orders of magnitude (10 nM to 1 mM) in a patient. In the case of infants, pharmacokinetic variability is generally even greater than with adults. Frequent monitoring of MTX concentration in serum is thus required. Typically, up to 7 samples are collected at different time points within 24 h after MTX administration to track its metabolism (Aumente et al., 2006). Because there is a defined relationship between treatment efficacy/toxicity and systemic drug exposure, MTX is a paradigm for a drug that provides better therapy with TDM in ensuring the

* Corresponding author at: Département de Chimie, Université de Montréal, C.P. 6128 Succ. Centre-Ville, Montréal, QC, Canada H3C 3J7. Fax: +1 514 343 7586.
E-mail address: jf.masson@umontreal.ca (J.-F. Masson).

http://dx.doi.org/10.1016/j.bios.2014.09.082
0956-5663/

efficacy and safety of the drug dose. In some cases, in order to decrease toxicity of the patient induced by MTX, folinic acid (leucovorin) rescue is undertaken by administering doses of folinic acid until serum MTX levels reach an acceptable concentration threshold. Depending on different patients, the safety threshold can be defined between 20 and 200 nM (Dasgupta, 2008).

MTX concentration is generally measured in clinical laboratories using either a Fluorescence Polarization Immunoassay Analyser (FPIA, TDx™, Abbott Laboratories), the ARK™ immunoassay (Ark Diagnostics, Inc.) or liquid chromatography coupled to tandem mass spectrometry (LC–MS/MS). The TDx™ analyser relies on the fluorescence polarization of labeled MTX bound to a monoclonal antibody, which is inversely proportional to the concentration of MTX in the sample. Fluorescence-labeled MTX is an expensive reagent and fluorescent biomolecules from blood can induce interference in FPIA measurements (AbbottLaboratories, 2009). The Ark MTX assay depends on the principle of enzyme multiplied immunoassay technique where glucose-6-phosphate dehydrogenase linked to the drug is rendered inactive for the reduction of nicotinamide adenine dinucleotide (NAD) when the labeled drug binds to the specific antibody. The spectral intensity change at 340 nm associated with the reduction of NAD is inversely proportional to the concentration of MTX (ArkDiagnostics, 2013). It has been reported that this method lacks precision especially at the lower concentration end of the calibration curve. For instance, the assay is not sensitive enough to analyze MTX concentrations near the safety threshold (50–200 nM) (Mendu et al., 2007). Nonetheless, both enzyme immunoassays offer generally high sensitivity, ease of use and fast MTX analysis. Lastly, LC–MS/MS is often the reference method used for MTX analyzes (Albertioni et al., 1996; Steinborner and Henion, 1999). However, LC–MS/MS is not suitable for most clinical laboratories requiring fast turnaround time since this technique is more expensive (cost of acquisition), time-consuming and labor intensive (due to sample preparation) and requires specialized operators. This explains the preference of clinical laboratories in employing routine immunoassays such as the TDx™ analyser for MTX quantification.

The ideal TDM tool for MTX should be more user-friendly than LC–MS/MS but at the same time comparable to FPIA in terms of cost effectiveness and analytical performance. Our proposed strategy is to employ a SPR biosensor offering simplicity, versatility, tunability and high sensitivity. We have recently reported a solution-based LSPR assay for MTX in clinical samples of patients undergoing chemotherapy (Zhao et al., 2012). The assay was based on the competition between MTX and folic acid-modified AuNP for binding to hDHFR in solution. The LSPR from the AuNP transduced binding of hHDFR to the folic acid-AuNP in absence of MTX. Due to the optical interference of serum with the LSPR of AuNP, solid phase extraction (SPE) of MTX in serum samples was required to analyze MTX in clinical samples. This procedure led to significant sample dilution, such that the assay had a dynamic range limited to the hundreds of nanomolar. A new transducer is thus required to improve sensitivity and dynamic range, and to avoid the use of SPE pre-treatment in the analysis of serum samples of patients. SPR can fulfill these requirements because the SPR light beam does not directly interact with the sample; the bioreceptor (hDHFR) can be immobilized on the surface using His-tag chemistry (Bolduc et al., 2011); and it is possible to miniaturize SPR instruments. The cost and bulkiness of most commercial SPR instruments, the lower analytical performance and deficiencies in terms of resolution of small SPR systems and the interference from nonspecific adsorption of biofluids have limited the use of SPR system in clinical laboratories (Breault-Turcot and Masson, 2012). To the best of our knowledge, there are no reported studies on SPR systems used in the clinical setting. Currently, commercially available SPR systems are not suited for clinical analysis due to high nonspecific adsorption or have not yet shown adaptability to the clinical environment.

Miniature SPR systems are desirable in clinical laboratories considering the limited bench space in clinical biochemistry laboratories and the high acquisition cost of most commercial SPR systems. Miniature SPR systems must incorporate all optical and electronic components into a single compact module. They must be easy to use with disposable sensing chips and integrated fluidics (Abbas et al., 2011). Background correction is common with suitable internal references (Homola, 2003). For instance, Texas Instruments Inc. has pioneered a portable SPR device with the development of SPREETA™, a small and inexpensive sensor of $1.5 \times 0.7 \times 3\ cm^3$. This instrument integrates all the SPR optical components into a molded and compact device (Marchesini et al., 2007; Naimushin et al., 2002). It was deployed for environment monitoring and bacterial detection (Marchesini et al., 2007; Naimushin et al., 2002). Recent appearance of miniature commercialized SPR devices include SPRmicro (K-MAC) (KMAC, 2012), SPIRIT (Seattle sensing systems) (Chinowsky et al., 2007), Smart SPR SS-1001 (Mebius advance technology) (NTT-AT, 2012) and Biosuplar 6 (Analytical μ-systems/Mivitec) (Biosuplar, 2012). Some challenges were identified which limit portable SPR systems with respect to gaining ground in biomedical applications. One involves the poorer resolution of portable systems, which is particularly important for analysis of small molecules. Secondly, portable SPR systems have not demonstrated examples of analysis in complex matrices as required for biomedical diagnostics in clinical settings. Lastly, small SPR systems were designed as dual-channel, while larger multiplexing has required several SPR instruments to be used in parallel. To address these challenges, we have designed a 4-channel miniature SPR system capable of performing the direct analysis of MTX in patients' serum during ongoing chemotherapy treatments.

2. Materials and methods

Detailed experimental procedures of the synthesis of the FA-AuNP, SPR sensor preparation and functionalization, expression of wild-type and mutant hDHFR, measurement of the interaction of FA-AuNP with hDHFR and processing of SPR signal are provided as electronic Supplementary information.

2.1. Multi-channel SPR system

The multi-channel system comprises 4 parallel light beams. This small and portable multi-channel SPR instrument was constructed based on light emitting diodes (LED), fiber optic-coupled collection of light, a small USB spectrophotometer (Ocean Optics USB4000 fiber optic spectrophotometer ranging from 467 to 727 nm), and custom-made microfluidics and electronics (Fig. 1). Each light beam was aligned on a channel of the SPR system. LEDs for each channel passed through a pinhole to remove diverging light, through a polarizer controlled with a rotation drive and the collimated light was collected with four 200-μm optical fibers. The fibers were merged into a linear array in a single SMA connector and aligned on the slit of the Ocean Optics spectrophotometer. The spectrophotometer was equipped with a focusing lens at the entrance of the spectrophotometer to focus light from each channel to the CCD array. Sequentially lighting the LEDs afforded interrogation of each channel without cross-talk. An electronic card was designed to control LED lighting, polarizer control and data acquisition from the spectrophotometer. A gold-coated dove prism (1 nm Cr and 45 nm Au) was deposited into the assigned cavity of the system; a disposable PDMS fluidic cell was placed on the prism and secured with a compressive latch. The sample and

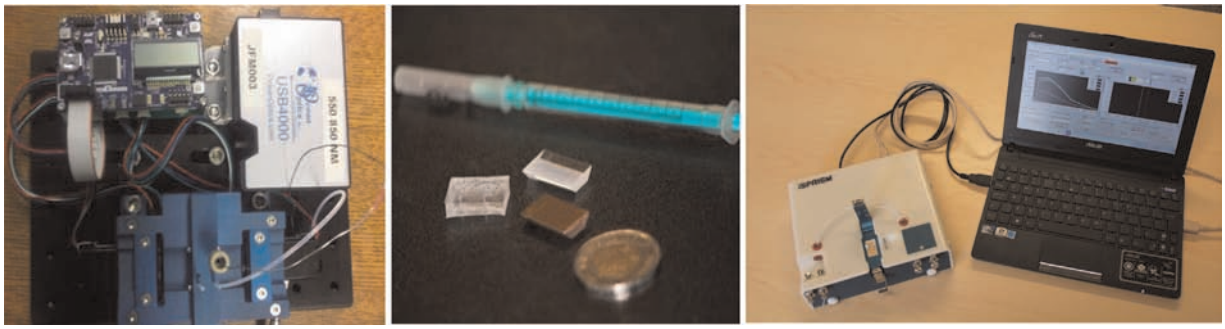

Fig. 1. (Left) Picture of the electronics and optics of the prototype system. Dimensions: 181 (*L*)x166 (*w*)x55 (*H*) mm^3. Weight: 1.3 kg. (Middle) Picture of a gold-coated Dove prism and PDMS fluidic cell. A Canadian 2$ coin and a 1 mL syringe show the scale. (Right) The SPR system is controlled by a 9″ laptop and requires no external power supply.

reference solutions are delivered to two different sensing areas by separate injection ports. The flow channel for sample analysis is S-shaped with a total volume of 16 μL. It covers three sensing areas on the prism, thus providing sample analysis in triplicate. The second flow channel has a volume of 5 μL. It covers the fourth sensing area and acts as a reference. Data acquisition was controlled by custom Labview software where the SPR signal was integrated at each time point using a minimum finding algorithm based on a second order polynomial fit of the SPR spectra. The Labview software allows users to set boundaries of the SPR data treatment for optimization of the noise level. The sensorgrams were displayed in real-time on the computer screen. All four traces are plotted in separate windows in the software and the three active channels can be background-corrected with the reference channel by toggling a box. The data was acquired sequentially for each channel with a speed of 10 accumulations per channel per second, with 90 ms integration time for each acquisition. Data output is saved as a text file for further data treatment with commonly available data analysis software (Matlab or Excel were used in these experiments).

2.2. Calibration of the MTX SPR sensor

The 3-MPA-LHDLHD-OH peptide SAM competent for binding His-tagged hDHFR was immobilized on gold-coated prisms on the SPR sensors as described in Supplementary information (ESI). This SAM has shown low fouling properties and is particularly suited for resisting nonspecific adsorption in crude serum for biomolecule quantification (Bolduc et al., 2011). The SPR sensors were mounted into the SPR system and conditioned for 5 min in 100 mM phosphate buffer (PB) at pH 8. In all cases, the solutions are injected in the fluidic cell and reacted under static flow conditions. Then, the biological receptor was immobilized by applying a 40 μg/mL hDHFR solution in PB for 10 min. PB was used for rinsing excess receptors for 5 min. Solutions containing different concentrations of MTX (10 pM to 100 μM) and a constant concentration of 13 nm FA-AuNP (1 nM) were injected on the SPR sensor for 15 min followed by rinsing for 5 min with PB. Data were processed using a minimum wavelength finding algorithm on Matlab to obtain the sensorgram. The binding shift was calculated from the sensorgram by subtraction of the last 50 data points of the PB steps before and after MTX sensing. By these means, competitive binding curves were established using 1 nM AuNP of 13 nm diameter, 0.5 nM AuNP of 23 nm diameter or 20 nM FA-AuNP of 5 nm diameter. The nature of the molecular receptor was also varied, using the wild-type (WT) or mutant (M) hDHFR with 1 nM FA-AuNP of 13 nm diameter. Note that the NP concentrations were chosen based on the volume ratio of the nanoparticle and the signal-to-noise ratio of the SPR signals in PBS. Normalization of the competitive binding curve was done against the response of the highest concentrations of MTX.

2.3. Analysis of MTX in clinical samples

The sensors were prepared as described above and the MTX analysis was carried with 1 nM of 23 nm FA-AuNP for 15 min. Control experiments were carried with samples containing only FA-AuNP. For the reference channel, the enzyme immobilization step was omitted by injecting buffer for that step. De-identified human serum samples were received from a local hospital (*Hôpital Maisonneuve-Rosemont*, Montreal, QC, Canada) and stored at −80 °C prior to MTX quantification. Six negative samples from a pool of healthy patients (no MTX treatment received) were provided for the construction of the calibration curve in human serum. The ethics committee (*Comité d'éthique de la recherche de l' Hôpital Maisonneuve-Rosemont*) has approved the experiments. All experiments were performed in compliance with the relevant laws and institutional guidelines. Since this study was classified as method development, informed consent was unnecessary. The appropriate concentration of MTX was spiked into different negative samples to construct the calibration curve. Clinical serum samples were thawed to room temperature immediately prior to analysis. The samples were mixed with 1 nM of 23 nm NP in 10 mM PB at a ratio of 1:10. The results of SPR analysis of the clinical samples were compared to those of FPIA and LC–MS/MS. The FPIA results were provided from the hospital laboratory, analyzed by an independent analyst. The LC–MS/MS results were acquired as described in a previous study (Zhao et al., 2012).

3. Results and discussion

3.1. Validation of the MTX competitive assay in buffered solutions

The SPR analysis for MTX depends on the competition between MTX and FA-AuNP for immobilized hDHFR (Scheme 1). Folic acid is a precursor molecule of dihydrofolate, the natural substrate of hDHFR. It has attracted great interest as a grafting material for gold nanoparticles in imaging and cancer cell targeting and therapy (Bhattacharyya et al., 2011; Chen et al., 2007). In this study, FA-AuNP was used as an amplification element to enhance the SPR signal. The binding of FA-AuNP to surface-bound hDHFR increases the refractive index change amplifying the SPR response. Different concentrations of MTX dictate the extent of FA-AuNP binding which in turn generates SPR response that can be correlated to MTX concentrations for assay calibration.

Comparing the interaction of 0.25 nM FA-AuNP and hDHFR in phosphate buffer (PB), in the absence and presence of MTX demonstrated the effectiveness of the MTX biosensor (see Fig. SI1). MTX binding was observed as a decrease of the SPR response of the interaction of FA-AuNP with hDHFR as a result of competitive binding of 100 nM MTX in a LSPR assay. A negative control in the absence of hDHFR was used to evaluate background response

of FA-AuNP and 100 nM MTX. No significant nonspecific response was observed in absence of hDHFR indicating low background. Specificity of the enzyme interaction with FA-AuNP was also demonstrated. MTX contains a glutamic acid (GA) group, which acts as the anchor point of FA onto the AuNP. The absence of LSPR response for GA-AuNP confirmed the specificity of the interaction between FA and hDHFR (Fig. SI1).

The solution-based LSPR sensor was adapted to the prism-based SPR system described above. To this effect, hDHFR was bound to a peptide monolayer competent for chelating histidine-tagged proteins, such as 6-His-tagged hDHFR (Fig. SI2). Using this protein attachment method to SPR sensors, Bolduc et al. (2011) and Ratel et al. (2013) demonstrated that hDHFR remains active when immobilized on a SPR sensor. The sensorgram showed that hHDFR binding in PB causes red shift of approximately 3 nm. The interaction between the hDHFR immobilized on the SPR sensor and the FA-AuNP further redshifted the plasmon resonance by approximately 3 nm. The SPR response with the FA-AuNP was calculated from the difference of PB response measured before and after the detection step. A control experiment was run for a SPR sensor without hDHFR (Fig. SI2). A small SPR response was measured for the detection step, indicating some nonspecific adsorption of the functionalized AuNP onto the surface. This value is considered as background signal and is subtracted from the specific binding response. Similarly to the LSPR colorimetric assay for MTX (Zhao et al., 2012), a dose–response curve was obtained for different MTX concentrations (Fig. 2). Due to the competitive nature of the assay, the SPR shift decreases for increasing concentrations of MTX. The reverse sigmoidal calibration curve illustrates the thermodynamic behavior of the affinity of the enzyme for the nanoparticle in the presence of different MTX concentrations (Fig. 2). For further quantification purposes, only the linear portion of the curve was considered.

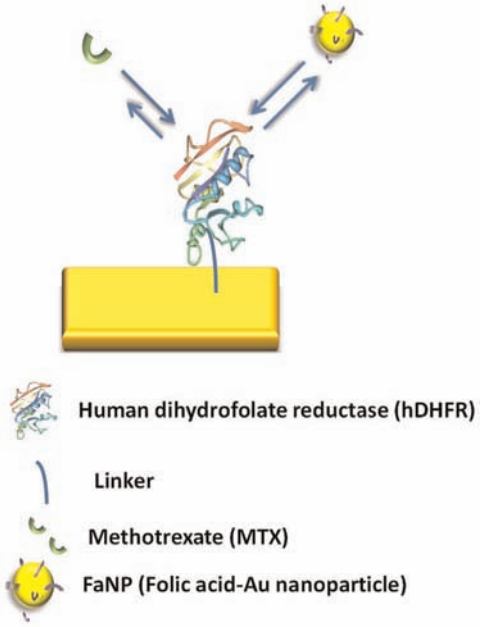

Scheme 1. Schematic illustration of the SPR competitive assay for MTX detection. A competition is established between MTX and FA-AuNP for binding to hDHFR that is immobilized to the surface of the SPR sensor.

3.2. Tuning the dynamic range of MTX calibration

3.2.1. Influence of NP size

The size of AuNP can influence several parameters in SPR assays, such as plasmonic coupling with the Au surface or the interactions with the bioreceptor. In this work, the effect of AuNP size on dynamic range of the competitive assay for MTX detection was explored since extended dynamic range is a requirement for this specific application. AuNP were synthesized with sizes of 5.2 ± 1.2, 13 ± 3.3 and 23 ± 5.1 nm. By varying the sizes of the NP, a modulation in the dynamic range of MTX detected is possible (Fig. 3). It is interesting to note that the sensitive range for MTX has shifted to smaller concentration with larger AuNP. The kinetics of the competitive assay may explain this observation. MTX diffuses to the sensor surface faster than do NP. As the size of NP increases, the diffusion coefficient also increases. By decreasing the FA-AuNP diameter nearly by a factor of two, from 23 to 13 nm, the competitive binding curve shifted towards the higher nM range. Using even smaller 5 nm NP, the dynamic range was shifted towards even higher concentrations, up to the μM range. Kinetically, 5 nm NP reach the sensor surface faster than 23 nm NP. A higher concentration of MTX is needed to compete with fast diffusing 5 nm NP. The final rinsing step does not significantly remove bound FA-AuNP or MTX molecules because the binding interaction with hDHFR is conducted in the kinetic-driven regime. Within the pre-determined detection time of 15 min, which is ideal for a clinical testing, the equilibrium has not yet reached steady state. Considering that MTX is a tight-binding inhibitor, the dissociation of MTX from hDHFR does not occur on the time scale

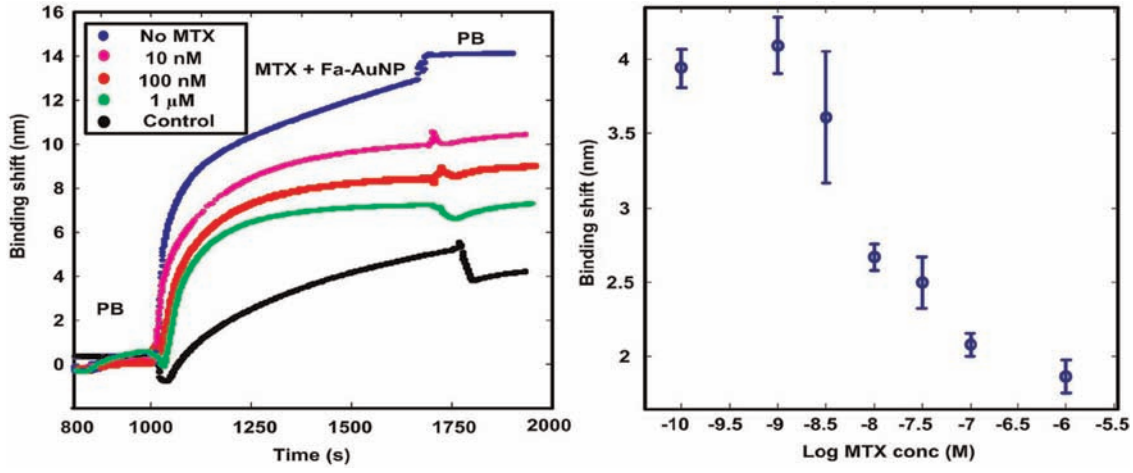

Fig. 2. (Left) MTX sensor response in PB, pH 8 with 0.04 mg/mL hDHFR, 2 nM FA-AuNP and varying concentrations of MTX. hDHFR was immobilized on the SPR sensor during the first 800 s. (Right) Competitive binding curve using 0.04 mg/mL hDHFR with 1 nM of FA-AuNP and varying concentrations of MTX. Error bars represent the standard deviation of a triplicate measurement.

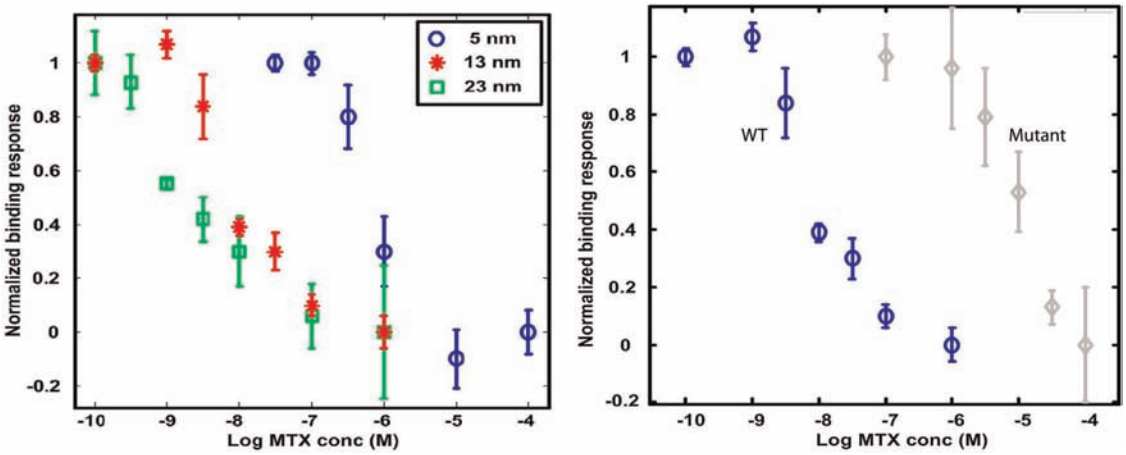

Fig. 3. (Left) Normalized MTX competitive binding curves using 0.04 mg/mL hDHFR with NP of different sizes in 10 mM PB, pH 8. (Right) Normalized MTX competitive binding curves using 0.04 mg/mL wild type (WT) and mutant hDHFR with 1 nM NP of 13 nm in 100 mM PB, pH 8. Error bars represent the standard deviation of a triplicate measurement.

of the experiments, which explains that the sensor is conducted in the kinetic regime.

Nonspecific adsorption also plays a major role in controlling the extent of the dynamic range. For competitive assay, high MTX concentrations should decrease the SPR shift to zero. However, in the case where nonspecific adsorption occurs, high MTX concentrations will lead to a SPR signal equal to the level of nonspecific adsorption. Thus, the upper limit of the linear range is reduced, masked by the nonspecific adsorption. We observed that increasing nonspecific adsorption accompanied decreasing size of FA-AuNP (Fig. SI3 A). Thus, the dynamic range was extended with larger AuNP due to lower nonspecific adsorption such that a lower detection limit could be attained. It is important to note that the SPR response observed due to NP binding was smaller for larger AuNP than the one induced by smaller sized NP during the same time frame (Fig. SI3 B). Depending on the requirement of dynamic range and detection limit for a specific application, the particle size can be optimized to maximize the analytical performance.

3.2.2. *Influence of hDHFR affinity for MTX*

Dynamic range in biosensing can be modulated by the affinity of the receptor for the analyte. Receptors with high affinity lead to lower detection limits. Volpato et al. have investigated the combination of active site mutations in hDHFR for increasing MTX resistance (Fossati et al., 2008; Volpato et al., 2009, 2011). Protein engineering was used to modify amino acids inside the active site to vary the enzyme's affinity for MTX. One particular hDHFR variant differs from the wild-type hDHFR (WT) by alteration of two amino acids responsible for MTX binding: phenylalanine 31 was mutated to arginine (F31R), and glutamine 35 was mutated to glutamic acid (Q35E). The resulting doubly-mutated hDHFR F31R/Q35E, hereafter referred to as mutant hDHFR, has 3 orders of magnitude lower affinity for MTX, with a K_I^{MTX} of 21 nM (Fossati et al., 2008) in comparison to WT hDHFR ($\leq$0.034 nM). It is interesting to highlight that the active site mutations did not influence protein folding so similar surface coverage is expected when coated on the gold film.

Sensor chips were coated with WT or mutant hDHFR and calibrations for MTX were compared using identical assay conditions of 1 nM of 13 nm FA-AuNP in 100 mM PB. The competitive binding curve was shifted towards higher concentration of MTX (1–30 μM) for the mutant DHFR (Fig. 3). As expected, the MTX-resistant mutant DHFR is sensitive to higher concentrations of MTX, leading to a shift in dynamic range of 3 orders of magnitude, equivalent to the difference in K_I^{MTX} between the WT and the mutant. These results demonstrate how differences in enzyme affinity can be used to modulate the dynamic range.

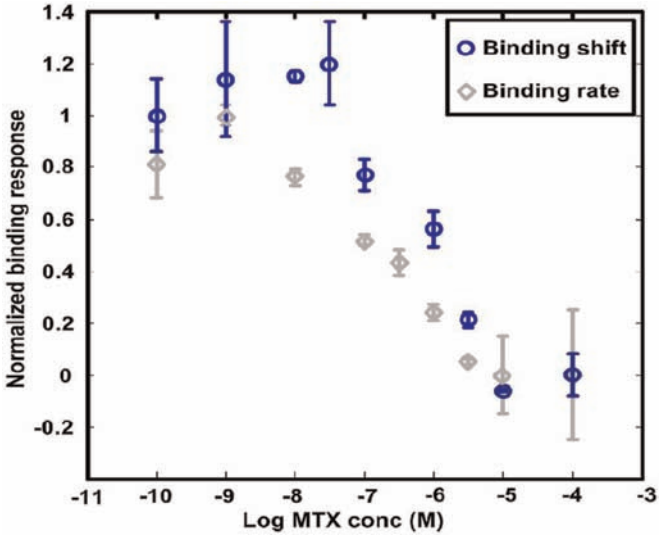

Fig. 4. Normalized MTX competitive binding curves using 0.04 mg/mL hDHFR with 1 nM NP of 5 nm in 100 mM PB, pH 8. Error bars represent the standard deviation of a triplicate measurement.

3.3. *Reducing the detection time*

Measuring the binding shift at equilibrium holds the advantage of yielding the largest possible SPR response, at the expense of analysis time. In contrast, measuring initial binding rates benefits from the rapid rise in SPR signal occurring in the first instants of detection to provide a rapid response. Springer et al. (2010) have shown quantitative analysis using both binding shift and initial binding rate parameters. Here, the initial binding rate was extracted from the data used for the SPR response at equilibrium. We observed that the initial binding rate was dependent on the concentration of MTX especially for low concentrations. Small molecules such as MTX diffuse more rapidly than FA-AuNP and can presumably access the binding pocket of hDHFR more readily than the bulky FA-AuNP. NP of 5 nm size were employed for this study since diffusion to the surface receptors is faster than for larger NP thus allowing a rapid response of the system.

The responses of the binding shift and rate generated with 5 nm AuNP for MTX analysis were normalized for comparison

(Fig. 4). It should be highlighted that the curve using the binding rate spans the same range of concentrations as the curve derived from the binding shift, and additionally extends slightly into lower MTX concentrations. This is explained by the fact that the data are not acquired at thermodynamic equilibrium. The thermodynamic model is used when the association and dissociation rates are equal, thus when the system is at equilibrium. At the time of injection of FA-AuNP and MTX onto the sensor surface, the binding sites are not saturated. As a result, association kinetics dominate and dissociation kinetics are negligible, such that the binding rate is proportional to the concentration of MTX. A linear relationship was established where increasing concentrations of MTX decrease the initial binding rate. This becomes an interesting aspect where results from two different parameters of the same dataset can be used for cross validation. Such data treatment allows rapid readout of the response under 60 s, which is extremely welcome for rapid analysis turnaround in clinical laboratories.

3.4. MTX calibration in human serum and clinical sample analysis

The analytical performance of the miniature multi-channel system was first evaluated in terms of sensitivity and resolution. Results show that the prototype system is comparable in RI sensitivity to other wavelength interrogation systems with resolution in the 10^{-6} RIU, which is similar to existing commercial miniaturized instruments. More details are found in Supplementary information section, as briefly summarized below.

The MTX competitive assay was validated using the miniature multi-channel system with measurements of two MTX concentrations (1 nM and 1 μM) in buffer. The real-time sensorgrams from all four sensing regions illustrate the measurement reproducibility (Fig. SI4). The sensorgrams demonstrated successful enzyme immobilization followed by indirect MTX analysis with FA-AuNP. The different magnitudes of response at 1 nM and 1 μM MTX showed that the system was sensitive to changes in MTX concentrations, as observed by the reduced binding shift at the higher MTX concentration. Nonspecific adsorption signal from the reference channel was subtracted from the test channels results.

Thereafter, the prototype system was applied to the calibration of MTX concentration in human serum. Sera from six different individuals were pooled and aliquots were spiked with MTX of varying concentrations. The sera samples were mixed at a 1:10 ratio with 10 mM PB, pH 6 containing the FA-AuNP. We recently found out that reducing the pH to 6 was more favorable to the interaction of the FA-AuNP with surface bound hDHFR (Bukar et al., 2014). Each sample was analyzed three times in triplicate (3 series of measurements with $n=3$; Fig. 5-Left). The coefficient of variation for triplicate analysis using multi-channel system varied from 5% to 26%. The variability in serum matrix composition poses a challenge for calibration and analysis in human serum, leading to large standard deviation in response. The reference channel eliminated the effect of the sample matrix and helped in isolating the specific binding signal for each serum sample. This shows the importance of referencing for complex matrix analysis. It is interesting to note that high MTX concentrations such as 1 μM still induced a response of 4 ± 1.8 nm. Theoretically, a zero response is expected since high concentration of MTX saturates all receptor sites such that no binding of FA-AuNP is possible. The residual background response may be explained by nonspecific adsorption of individual or clusters of FA-AuNP via electrostatic interactions with the enzyme on the surface. The reference channel, in the absence of the enzyme coating, is less susceptible to nonspecific adsorption of FA-AuNP.

The linear portion of the calibration curve (Fig. 5-Left) was used to analyze 6 clinical samples in different concentration ranges (Fig. 5-Right). The dilution factor needs to be taken into account because the samples are diluted 10-fold before the analysis. The dynamic range was estimated to extend to 500 nM with a limit of detection of 28 nM. Samples were further diluted if the concentration was determined to be larger than 500 nM. In comparison, our previous LSPR sensor had a detection limit of 155 nM with a dynamic range extending to 360 nM in serum samples (Zhao et al., 2012). The current SPR assay showed a greater dynamic range and better detection limit. The dynamic range will be amenable to tuning toward higher concentration ranges by using smaller NP and/or mutant hDHFR (Fig. 3). The results from SPR sensing were compared to those given by FPIA and LC–MS/MS (Fig. 5). Samples 1, 3 and 5 were successfully identified as samples with MTX concentrations in the μM range. Samples 2 and 6 were evaluated as samples with concentration <1 μM, in the nM range. Sample 4 is a blank (no MTX) but was identified as a sample with low nM concentration of MTX with both the SPR and LC–MS/MS.

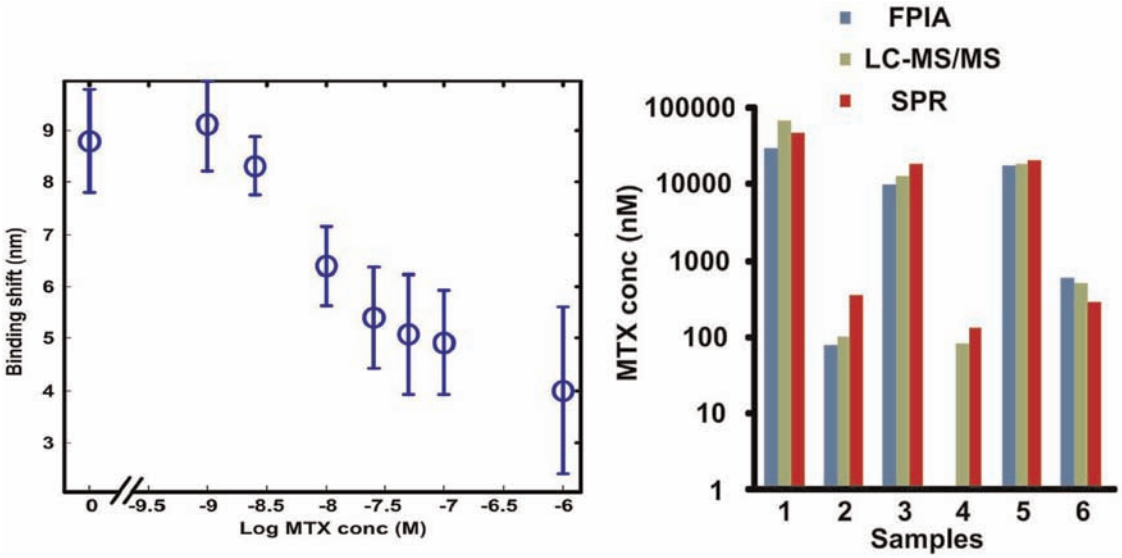

Fig. 5. (Left) Calibration in human sera of the MTX assay using 1 nM of 23 nm FA-AuNP mixed in a 1:10 ratio with 10 mM PB, pH 6, using the 4-channel, fully integrated SPR system. (Right) Comparative analysis of MTX-containing clinical samples using FPIA (blue; bars to the left), LC–MS/MS (green; bars in the center) and SPR (red; bars to the right). (For interpretation of the references to color in this figure legend, the reader is referred to the web version of this article.)

3.5. System performance in a clinical setting

The miniature multi-channel SPR system was installed in the clinical laboratory of the Biochemistry department at the *Hôpital Maisonneuve-Rosemont* (Fig. SI5) for testing with novice users. The MTX assay calibration (Fig. SI6) and system resolution (Fig. SI7) in the clinical setting were comparable to the results obtained in a controlled environment laboratory. In addition, three new users were invited to repeat the same analysis as two experienced users. First, two samples of the same MTX concentration were repeated by user one. The results from three different sensing areas of both analyzes were reproducible. The same analysis was conducted by a second user. The coefficients of variation (CV) were comparable independently of experienced or new users (Fig. SI8). The measurements were achieved with a CV of 9–23% for analysis of the control test (0 MTX) and 6–16% for 50 μM MTX as shown from the single day analysis with multiple users (one new and one experienced). It can be concluded that the system can be operated by inexperienced users without extensive training. The miniature SPR system has shown clinical adaptability in a clinical biochemistry laboratory. The analytical performance of the MTX assay and system performance did not change as a result of deployment. Reproducibility of the system was proven, as the data generated from new clinical users with basic training (clinical staff at Maisonneuve-Rosemont hospital) was equivalent to trained users (authors of the paper).

4. Conclusions

A SPR competitive assay was successfully established for the analysis of MTX in human serum. Variation in NP sizes as well as hDHFR affinity modulated the dynamic range. The initial binding rate data offered rapid sensor response. Furthermore, the applicability of the multi-channel system was demonstrated through the adaptation of the MTX competitive assay. Its sensor performance and ability to be employed in the clinical laboratory proves its prospective application in its designated context. The system performance is no different upon deployment. The calibration conducted in the research laboratory was reproduced in the clinical setting. The reproducibility amongst users is satisfactory since new and experienced users generated results with similar coefficient of variation. With these encouraging results, the next milestone would be to prove the point-of-care capacity of the prototype system at the bedside of the patients. Portable SPR devices hold great promise in future clinical diagnostics and will continue to be the rising star in point-of-care biosensing devices technologies.

Acknowledgments

The authors acknowledge Doris Vandal, Annie Ducharme and Eric Patenaude St-Pierre from Maisonneuve-Rosemont Hospital for their participation in the clinical evaluation of the SPR system. The authors also acknowledge financial support of the National Sciences and Engineering Research Council of Canada (grant number I1IPJ 430-487-12 and 341972-2011) the Centre for Self-assembled Chemical Structures (CSACS), the Fonds de Recherche du Québec Nature et Technologies (FRQ-NT) (grant number 2010-PR-140186) and the Institut Mérieux.

Appendix A. Supplementary information

Supplementary data associated with this article can be found in the online version at http://dx.doi.org/10.1016/j.bios.2014.09.082.

References

Abbas, A., Linman, M.J., Cheng, Q., 2011. Biosens. Bioelectron. 26 (5), 1815–1824.
AbbottLaboratories, 2009. TDX/TDXFLX-Methotrexate II—Technical ManualAbbott Laboratories Diagnostic division, Abbott Park, IL.
Ackland, S.P., Schilsky, R.L., 1987. J. Clin. Oncol. 5 (12), 2017–2031.
Albertioni, F., Rask, C., Eksborg, S., Poulsen, J.H., Pettersson, B., Beck, O., Schroeder, H., Peterson, C., 1996. Clin. Chem. 42 (1), 39–44.
ArkDiagnostics, 2013. http://www.ark-tdm.com/pdfs/AACC2011Methotrexate_11 × 17.pdf, (accessed 02.10.13).
Aumente, D., Buelga, D.S., Lukas, J.C., Gomez, P., Torres, A., Garcia, M.J., 2006. Clin. Pharmacokinet. 45 (12), 1227–1238.
Bhattacharyya, S., Kudgus, R.A., Bhattacharya, R., Mukherjee, P., 2011. Pharm. Res. 28 (2), 237–259.
Biosuplar, 2012. ⟨http://www.biosuplar.de/⟩ (accessed 16.12.12).
Blum, R., Seymour, J.F., Toner, G., 2002. Ann. Oncol. 13 (2), 327–330.
Bolduc, O.R., Lambert-Lanteigne, P., Colin, D.Y., Zhao, S.S., Proulx, C., Boeglin, D., Lubell, W.D., Pelletier, J.N., Fethiere, J., Ong, H., Masson, J.-F., 2011. Analyst 136 (15), 3142–3148.
Breault-Turcot, J., Masson, J.-F., 2012. Anal. Bioanal. Chem. 403 (6), 1477–1484.
Bukar, N., Zhao, S.S., Charbonneau, D.M., Pelletier, J.N., Masson, J.-F., 2014. Chem. Commun. 50 (38), 4947–4950.
Chen, Y.H., Tsai, C.Y., Huang, P.Y., Chang, M.Y., Cheng, P.C., Chou, C.H., Chen, D.H., Wang, C.R., Shiau, A.L., Wu, C.L., 2007. Mol. Pharm. 4 (5), 713–722.
Chinowsky, T.M., Soelberg, S.D., Baker, P., Swanson, N.R., Kauffman, P., Mactutis, A., Grow, M.S., Atmar, R., Yee, S.S., Furlong, C.E., 2007. Biosens. Bioelectron. 22 (9–10), 2268–2275.
Dasgupta, A., 2008. Handbook of Drug Monitoring Methods. Humana Press Inc., Totowa, NJ.
Fossati, E., Volpato, J.P., Poulin, L., Guerrero, V., Dugas, D.A., Pelletier, J.N., 2008. J. Biomol. Screen. 13 (6), 504–514.
Graf, N., Winkler, K., Betlemovic, M., Fuchs, N., Bode, U., 1994. J. Clin. Oncol. 12 (7), 1443–1451.
Homola, J., 2003. Anal. Bioanal. Chem. 377 (3), 528–539.
KMAC, 2012. ⟨http://www.kmac.to/eng/product/php?cid=sprlab⟩ (accessed 16.12.12).
Marchesini, G.R., Koopal, K., Meulenberg, E., Haasnoot, W., Irth, H., 2007. Biosens. Bioelectron. 22 (9–10), 1908–1915.
Mendu, D.R., Chou, P.P., Soldin, S.J., 2007. Ther. Drug Monit. 29 (5), 632–637.
Naimushin, A.N., Soelberg, S.D., Nguyen, D.K., Dunlap, L., Bartholomew, D., Elkind, J., Melendez, J., Furlong, C.E., 2002. Biosens. Bioelectron. 17 (6–7), 573–584.
NTT-AT, 2012. ⟨http://www.ntt-at.com/products_e/handy_spr/⟩ (accessed 16.12.12).
Pignon, T., Lacarelle, B., Duffaud, F., Guillet, P., Catalin, J., Durand, A., Monjanel, S., Favre, R., 1994. Cancer Chemother. Pharmacol. 33 (5), 420–424.
Ratel, M., Provencher-Girard, A., Zhao, S.S., Breault-Turcot, J., Labrecque-Carbonneau, J., Branca, M., Pelletier, J.N., Schmitzer, A.R., Masson, J.F., 2013. Anal. Chem. 85 (12), 5770–5777.
Springer, T., Piliarik, M., Homola, J., 2010. Anal. Bioanal. Chem. 398 (5), 1955–1961.
Steinborner, S., Henion, J., 1999. Anal. Chem. 71 (13), 2340–2345.
Volpato, J.P., Yachnin, B.J., Blanchet, J., Guerrero, V., Poulin, L., Fossati, E., Berghuis, A. M., Pelletier, J.N., 2009. J. Biol. Chem. 284 (30), 20079–20089.
Volpato, J.P., Mayotte, N., Fossati, E., Guerrero, V., Sauvageau, G., Pelletier, J.N., 2011. J. Mol. Recognit. 24 (2), 188–198.
Walling, J., 2006. Invest. New Drugs 24 (1), 37–77.
Zhao, S.S., Bichelberger, M.A., Colin, D.Y., Robitaille, R., Pelletier, J.N., Masson, J.F., 2012. Analyst 137 (20), 4742–4750.